14

Remarks on the Use of ^{13}C and ^{18}O Isotopes in Atmospheric CO_2 to Quantify Biospheric Carbon Fluxes

Philippe Ciais, Matthias Cuntz, Mark Scholze, Florent Mouillot, Philippe Peylin, Vincent Gitz

Introduction

In this review chapter, we write the mass-conservation equations for CO_2 and its isotopomers $^{13}CO_2$ and $CO^{18}O$ that can be used to infer globally biospheric and oceanic net fluxes in the case of ^{13}C, and gross terrestrial biospheric fluxes in the case of ^{18}O. The quantitative use of atmospheric measurements of ^{13}C and ^{18}O in CO_2 to better constrain those fluxes requires knowledge of various processes specific to each isotopomer. The chapter is divided into two parts, one on each isotope. For ^{13}C, we review existing work that calculated isofluxes either using global estimates, or derived isofluxes from spatially and temporally explicit models. In addition, we estimate the magnitude of new isofluxes that were not addressed in former studies. These cover the effects of biomass burning, rock weathering and volcanism, and the oxidation of reduced carbon gases into CO_2 within the atmosphere. We also performed a new global calculation of the ^{13}C isoflux caused by the replacement of C_3 vegetation by C_4 plants following changes in land use. Those isotopic disequilibrium terms which roughly correspond to a ^{13}C flux to or from the atmosphere that has no counterpart in ^{12}C, prove to be important in the global apportionment of ocean vs terrestrial carbon fluxes using atmospheric ^{13}C data. Altogether, they have an aliasing effect of up to 1 $GtC\,yr^{-1}$. For ^{18}O, which is less understood than ^{13}C, we discuss in detail the different processes and controlling variables that contribute to the atmospheric signal. To do so, we refer to the calculations of spatially explicit global models of the soil–plant–atmosphere system. In the specific case of ^{18}O, the isotopic disequilibrium terms

are of secondary importance because ^{18}O directly constrains the gross fluxes (photosynthesis and ecosystem respiration) rather than the net fluxes as for ^{13}C. One exception to that rule is the disequilibrium induced by stratosphere–troposphere mixing of the enriched stratospheric ^{18}O signal.

Formulation of Global Budgets

Globally, the change of CO_2 in time is the sum of all surface fluxes, F_i:

$$\frac{dC_a}{dt} = M_a \sum_i F_i \tag{14.1}$$

where C_a denotes the global mean atmospheric CO_2 mixing ratio and M_a the conversion factor between fluxes in GtC and mixing ratios in ppm. $1/M_a = 2.12\,\mathrm{GtC\,ppm^{-1}}$, i.e., about 2 GtC are required to change the atmospheric CO_2 mixing ratio by 1 ppm (M_a is independent of the CO_2 mixing ratio). The same equation can be used for the relationship of the mixing ratio of an isotopomer of CO_2, for example, like $^{13}CO_2$ or $CO^{18}O$ (a plain C stands thereby for ^{12}C and a plain O stands for ^{16}O), with the surface fluxes of the isotopomer. Denoting all isotopomer variables with a prime gives:

$$\frac{dC'_a}{dt} = M_a \sum_i F'_i \tag{14.2}$$

R_x is the ratio of C'_a over C_a or of F'_i over F_i, so Eq. 14.2 can be written as:

$$\frac{d(C_a R_a)}{dt} = M_a \sum_i R_i F_i \tag{14.3}$$

Writing this in delta notation, $\delta = R_x/R_{standard} - 1$, and using Eq. 14.1 gives:

$$\frac{d(C_a \delta_a)}{dt} = M_a \sum_i \delta_i F_i \tag{14.4}$$

with δ_a the global mean atmospheric delta value of CO_2 and δ_i the delta value of the CO_2 flux, *i*. $C_a\delta_a$ is thereby a mass conservative tracer, just like CO_2. $dC_aR_a = R_a dC_a + C_a dR_a$, so Eq. 14.3 can be written as:

$$C_a \frac{dR_a}{dt} = M_a \sum_i R_i F_i - R_a M_a \sum_i F_i = M_a \sum_i F_i (R_i - R_a) \tag{14.5}$$

Or in delta notation:

$$\frac{d\delta_a}{dt} = \frac{M_a}{C_a} \sum_i F_i (\delta_i - \delta_a) = \frac{M_a}{C_a} \sum_i F_i \Delta_i \tag{14.6}$$

Δ_i is therefore just the difference between the delta value of flux i and the atmospheric delta value. The product of F_i and Δ_i is called isoflux, so the temporal evolution of CO_2 is mainly the sum of all CO_2 fluxes and the evolution of the atmospheric delta value is the sum of all isofluxes. Conceptually, the index i in Eqs 14.1 and 14.2 need not be the same. That means that the net flux of a process for CO_2 can be zero but there can be a flux of the isotopomer. For example, the ocean in steady-state gives a zero net flux of CO_2 but it can absorb $^{14}CO_2$, changing the delta value of ^{14}C in atmospheric CO_2 without changing the atmospheric CO_2 mixing ratio. In this case, one writes the zero net CO_2 flux as two canceling CO_2 gross fluxes in Eq. 14.6. Here 'canceling' means that both $F_{i,in}$ and $F_{i,out} = -F_{i,in}$ would appear as F_i in Eq. 14.1. More generally, if we group all canceling gross fluxes F_j in Eq. 14.6, it changes to:

$$\frac{d\delta_a}{dt} = \frac{M_a}{C_a}\left[\sum_i F_i(\delta_i - \delta_a) + \sum_j F_j(\delta_{j,in} - \delta_{j,out})\right]$$
$$= \frac{M_a}{C_a}\left(\sum_i F_i \Delta_i - \sum_j D_j\right) \tag{14.7}$$

where F_i are resulting net (for ^{13}C) or gross (for ^{18}O) fluxes that appear also in Eq. 14.1, and D_j values are called 'isotopic disequilibria' and are the product of the CO_2 gross flux and the difference between the delta value of the gross flux into and out of the atmosphere. The D_j values stay unchanged if one regards the mass conservative tracer $C_a\delta_a$ and Eq. 14.4 becomes:

$$\frac{d(C_a\delta_a)}{dt} = M_a\left(\sum_i \delta_i F_i + \sum_j D_j\right) \tag{14.8}$$

In the text below, we will suppress M_a and M_a/C_a for simplicity. This is the same as expressing the CO_2 fluxes and isofluxes in the correct units.

Understanding $\delta^{13}C$ in Atmospheric CO_2

Atmospheric ^{13}C is fractionated by C_3 terrestrial photosynthesis ($\sim -17‰$) with only minor effects caused by air–sea gas exchange processes ($\sim -2‰$). On the other hand, C_4 plants fractionate very little ($\sim -4.4‰$), and therefore C_4 plant exchange of carbon with the atmosphere cannot be distinguished from air–sea fluxes. Atmospheric measurements of ^{13}C and CO_2 have been used to apportion ocean and land fluxes globally with their year-to-year fluctuations, using time series from few stations (Francey *et al.*, 1995; Keeling, 1995), and regionally using a network of stations and atmospheric

tracer transport models (Heimann and Keeling, 1989; Ciais *et al.*, 1995a,b; Fung, 1997; Bousquet, 1999a,b; Rayner *et al.*, 1999). This method, called 'double deconvolution' has also been applied to ice-core records of CO_2 and $\delta^{13}C$ to reconstruct the temporal evolution of ocean and land net fluxes over the twentieth century (Joos and Bruno, 1998; Trudinger *et al.*, 1999). The double deconvolution is based on the mass balance of CO_2 and $^{13}CO_2$ in the atmosphere. The mass balance of CO_2 can be expressed as:

$$\frac{dC_a}{dt} = F_o + F_b + F_f \tag{14.9}$$

where F_o and F_b are the netalgebraic air–sea fluxes and air–land fluxes, and F_f represents the fossil fuel emissions. The F_b term can be broken down into:

$$F_b = F_{bur} + F_{bur\_regrow} + F_{def\_resp} + F_{def\_assim} + F_{res} \tag{14.10}$$

where F_{bur} is the CO_2 source implied by biomass burning that is partially offset by a carbon sink due to re-growth over burned areas F_{bur_regrow}. F_{def_resp} is the gross loss of carbon to the atmosphere implied by forest conversion to either grasslands or pastures, and F_{def_assim} is the gross carbon uptake due to re-growth of newly established ecosystems following deforestation. F_{res} is the residual terrestrial flux, globally a sink, which is often referred to as the 'missing sink' of anthropogenic CO_2. The mass balance of atmospheric ^{13}C is given by:

$$\frac{d\delta_a}{dt} = F_o \cdot \varepsilon_{ao} + F_b \cdot \Delta_b^{13} + F_f \cdot (\delta_f - \delta_a) + D_o + D_b + D_{bur} + D_{def} \tag{14.11}$$

where Δ_b^{13} is the average ^{13}C discrimination of terrestrial plants and ε_{ao} is the sea-to-air isotopic fractionation factor. The last four terms on the right hand side are called isotopic disequilibria, and their expressions are given by:

$$D_o = F_{ao} \cdot (\delta_o - \delta_o^e) \tag{14.12}$$

$$D_b = F_{HR} \cdot (\delta_b - \delta_b^e) \tag{14.13}$$

$$D_{bur} \approx F_{bur} \cdot (\delta_{bur} - \delta_{bur\_regrow}) \tag{14.14}$$

$$D_{def} = F_{def\_resp} \cdot (\delta^*_{def\_resp} - \delta^*_{def\_assim}) \tag{14.15}$$

where the subscript *HR* represents heterotrophic respiration. The disequilibria have in common that they cause a net flux of δ to or from the atmosphere in Eq. 14.11, with no counterpart in the net CO_2 fluxes in Eq. 14.9. Thus, isotopic disequilibria are very important terms in double deconvolutions, which must be estimated in order to properly infer F_b and F_o separately from atmospheric measurements. Both isoflux terms and isotopic

disequilibria terms, expressed globally in Eqs 14.11–14.15, are spatially distributed of course. If we are to use transport models instead of a single-box atmosphere, then the spatial and temporal distribution of the disequilibria flux must be estimated and subsequently transported to be accounted for (for instance pre-subtracted) in the $\delta^{13}C$ signal at atmospheric stations. The isotopic disequilibria are generally proportional to the gross exchange fluxes, with the exception of fossil fuel emissions. In the following sections, we review the magnitude of the isotopic disequilibria, their uncertainty at the global scale, and wherever possible their spatial distribution. Finally in the last paragraph, we focus our attention on spatial and temporal patterns of plant discrimination.

Air–Sea Isotopic Disequilibrium (D_o)

The air–sea ^{13}C disequilibrium is proportional to the sea-to-air gross flux, $F_{oa} = K_{ex} p_o$, and hence its estimation requires knowledge of the CO_2 partial pressure in surface waters (p_o) and the air–sea gas transfer coefficient K_{ex}. The air–sea disequilibrium therefore bears an uncertainty at least as large as that of the air–sea gas exchange transfer coefficient [±30% (Wanninkhof, 2002)]. It is also noted that F_{oa} increases with time along with the secular atmospheric increase in CO_2, as over most ocean gyres, p_o tracks the atmospheric partial pressure signal p_a. Today's average value of F_{oa} is on the order of 85 ± 17 GtC yr^{-1} (Heimann and Maier-Reimer, 1996). It should be pointed out (Joos and Bruno, 1998) that modeling D_o requires an estimation of p_o, and K_{ex} and thus is not independent of inferring the net air–sea flux $F_o = K_{ex}(p_o - p_a)$. The sea-to-air flux has already increased by roughly 30% since preindustrial times and will likely continue to do so in the future, making the air–sea disequilibrium a dominant term in future double deconvolutions. The difference between δ_o, the real world ocean $\delta^{13}C$ in surface waters total carbon and the hypothetical value that would correspond to isotopic equilibrium with today's atmosphere $\delta_o^e = \delta_a - \varepsilon_{ao} + \varepsilon_{oa}$, is positive. Indeed, ocean carbon integrates atmospheric ^{13}C that has invaded the ocean earlier on, when atmospheric $\delta^{13}C$ was higher than today because of the secular decrease in atmospheric $\delta^{13}C$ due to fossil fuel accumulation in the atmosphere. Estimates of the $\delta_o - \delta_o^e$ difference of 0.43‰ made by Tans *et al.* (1993) using earlier ocean data has been revised by Gruber and Keeling (2001) to 0.62 ± 0.08‰, based on more recent oceanographic surveys, which makes the overall air–sea disequilibrium term on the order of 53 ± 13 GtC ‰ yr^{-1}. Other published estimates are 47 GtC ‰ yr^{-1} using a 3-D ocean carbon model (Murnane and Sarmiento, 2000), and 60 GtC ‰ yr^{-1} using a reduced ocean model (Joos *et al.*, 1999), and 50 GtC ‰ yr^{-1} using latitudinal averages of ocean $\delta^{13}C$ data and gas transfer coefficient fields (Ciais *et al.*, 1995b; Battle *et al.*, 2000). In comparison, in

Eq. 14.11 a 1 GtC yr^{-1} sink in C_3 biomes ($\varepsilon_{ab} = -17‰$; $\delta_a = -8‰$) would increase δ_a by 25 GtC ‰ yr^{-1}.

Soil-Respired Isotopic Disequilibrium (D_b)

The soil-respired isotopic disequilibrium is proportional to the return flux of CO_2 from land ecosystems to the atmosphere F_{ba}. Strictly speaking, if F_{ab} equals net carbon assimilation, then F_{ba} equals ecosystem respiration. Generally, averaged over long enough timescales (longer than a few weeks) the difference in isotopic composition between assimilates incorporated by plant photosynthesis and their respiration by maintenance and growth respiration is close to zero. This assumption seems reasonable in light of isotope marking experiments (Ekblad and Högberg, 2001), but measurements over sub-daily periods suggest that assimilation and ecosystem respiration rarely reach isotopic equilibrium (Bowling *et al.*, 1999, 2001; Ogée *et al.*, 2003), except perhaps during the early morning and late afternoon. Yet assuming isotopic equilibrium between CO_2 respired by autotrophic processes and CO_2 fixed by photosynthesis, F_{ab} can be identified to net primary productivity (*NPP*) and thereof F_{ba} to heterotrophic respiration F_{HR}. As remarked for the air–sea disequilibrium, F_{HR} is not strictly independent of the 'unknown' F_b in Eq. 14.11, since $F_b = -NPP + F_{HR}$ ignoring disturbances, hence introducing another degree of complexity in modeling the soil-respired isotopic disequilibrium, D_b. Since the globally averaged net biospheric flux F_b generally amounts to a small fraction (only 1–2% of the gross flux F_{HR}), one can make for global studies the reasonable assumption that $F_{HR} \approx NPP$. This simplification is not verified regionally at the scale of current atmospheric inversions, or at the stand scale. For instance, one can compare regional *NPP* estimates from models (Cramer *et al.*, 2001) and *NBP* from inversions (Gurney *et al.*, 2002) at the scale of continents, or *NPP* and *NEP* values at stand level (Valentini *et al.*, 2000; Wirth *et al.*, 2002) to realize that F_b may be regionally or locally a sizeable fraction of *NPP*. Third, the value of the soil-respired disequilibrium D_b should increase with time as the input of carbon to ecosystems via *NPP* may increase to yield a net uptake of carbon in ecosystems. If *NPP* has globally increased as driven by CO_2 fertilization (Thompson *et al.*, 1996) or by other factors (Nemani *et al.*, 2003) over the past decades, then D_b must have paralleled the trend in *NPP*. Today's estimate of global F_{HR} ranges from 39.9 to 80.5 GtC yr^{-1} if based on *NPP* from 15 global models (Cramer *et al.*, 1999) and is 76.5 GtC yr^{-1} based on soil respiration measurements (Raich and Potter, 1995). This latter estimate is 30 to 60% higher than global *NPP* because it takes into account root autotrophic respiration of recent assimilates, which would make it inappropriate to estimate the global isotopic disequilibrium D_b. The isotopic difference between soil-respired CO_2 issued from organic matter decomposition and

recently formed phytomass (δ_p^e) depends on the turnover time of excess carbon in ecosystems, which increases with increasing latitude and decreasing temperatures (Schimel *et al.*, 1994). Note again that turnover times of carbon are not independent from the inferred biospheric uptake F_b in double deconvolutions (Randerson *et al.*, 1998). The difference in isotopic composition $\delta_b - \delta_p^e$ between newly formed phytomass and soil-respired CO_2 from previously formed biomass has been evaluated at 0.5‰ (Heimann and Keeling, 1989) and 0.5‰ (Ciais *et al.*, 1995a) using zonally averaged turnover times, and 0.56‰ (Ciais *et al.*, 1999), 0.33‰ (Fung *et al.*, 1997) and 0.53‰ (Scholze *et al.*, 2003) using spatially explicit global biosphere models. These numbers correspond to a flux-weighted global average. The value of $\delta_b - \delta_p^e$ is generally higher in biosphere models at high northern latitudes where a long residence time of carbon in soils prevails, and in tropical forests where carbon is immobilized in long-lived trees. To our knowledge, few measurements of $\delta_b - \delta_p^e$ are available, but it should be kept in mind that, generally, most newly formed biomass gets respired rapidly, and thus bears only a small isotopic disequilibrium. For instance, using radiocarbon tracing methods, Balesdent and Recous (1997) determined that over a tilled temperate cropland, 75% of the litter is degraded within a year, whereas 14% of soil carbon had a residence time of 40 years. Gaudinski *et al.* (2000) at Harvard Forest suggest that 59% of soil respiration was issued from carbon that resided in the plant/soil pools for less than a year, with an average of CO_2 produced by heterotrophs of 8 years only. It should finally be noted that there must be seasonal variations in $\delta_b - \delta_p^e$, in the range of 0.3‰ as modeled by Fung *et al.* (1997, see their Fig. 7) as different pool sizes are seasonally degraded by respiration processes. Together with estimates of heterotrophic respiration, the global soil-respired isotopic disequilibrium D_b ranges from 19.8 GtC ‰ yr^{-1} (Fung *et al.*, 1997) to 33.6 GtC ‰ yr^{-1} (Ciais *et al.*, 1999) and 37.4 GtC ‰ yr^{-1} as the mean over the 1990s (Scholze *et al.*, 2003).

Biomass Burning Isotopic Disequilibrium (D_{bur})

The isotopic composition δ_{bur} of burned aged biomass is isotopically enriched compared to recently formed plant tissues in recovering ecosystems after fire (δ_{bur_regrow}). Assuming $\delta_{bur} = \delta_{bur\_regrow}$, this would yield to aliasing towards a higher terrestrial sink in double deconvolutions. We used the historical record of atmospheric $\delta^{13}C$ together with estimates of the mean age of burned biomass (from fire return times) and combustion fluxes to estimate the value $\delta_{bur} = -7.55$‰, that is, 0.45‰ heavier than for today's atmosphere. Overall, it is difficult to compute the net imbalance in the terrestrial carbon budget implied by biomass burning sources, partly offset by post-fire recovery sinks. Assuming that $F_{bur} = F_{bur\_regrow}$

(range 2.1–3.4 GtC yr^{-1}) yields a biomass burning disequilibrium isoflux $D_{bur} = 1.66$ GtC ‰ yr^{-1}. That is a small contribution to the mean trend in $\delta^{13}C$, equivalent to aliasing a terrestrial sink of 0.1 GtC yr^{-1}.

Isotopic Effects Caused by Land Use and C_3/C_4 Shifts in Vegetation

The conversion of forests to croplands and grasslands globally decreases the turnover time of carbon in ecosystems and thus acts to reduce the value of the soil-respired disequilibrium. In addition, in places where forests are converted to C_4 crops (e.g., sugar cane) or C_4 pastures, a difference in isotopic composition between newly formed C_4 biomass and respired CO_2 from former C_3 forest soils, of the order of $\Delta_{b-C_4} - \Delta_{b-C_3} \approx 12.5‰$, will be seen in the atmosphere. This disequilibrium term, D_{def}, unlike the ocean and the soil-respired disequilibria D_o and D_b, acts to deplete the atmosphere of ^{13}C. Ignoring it would be equivalent to inferring too small a terrestrial sink F_b in double deconvolution studies. The land use disequilibrium accounts for a source of CO_2 to the atmosphere right after forest conversion followed by delayed emissions during the release of former C_3 soil carbon, the sum of both being F_{def_resp}, which is counterbalanced by carbon uptake from the newly established vegetation F_{def_assim}. After all former C_3 soil carbon has been oxidized, a new carbon equilibrium state is reached, which is also a carbon isotopic equilibrium state, where inputs compensate for outputs. Typically this takes 20 to 30 years in the tropics (Townsend *et al.*, 1997). The global significance of this effect, outlined by Ciais *et al.* (1999), was quantified by Townsend *et al.* (2002) using the CENTURY soil carbon model. Over all fractions of land that have been converted during a time period beginning τ years ago until today, the land use change-induced isotopic disequilibrium at instant t is:

$$D_{def}(t) = \int_{u=t-\tau}^{u=t} F_{def\_resp}\,\delta_{def\_resp}\,du - \int_{u=t-\tau}^{u=t} F_{def\_assim}\,\delta_{def\_assim}\,du \tag{14.16}$$

This equation is unpleasant to account for because it would mean that F_b alone cannot be solved separately in Eqs 14.9 and 14.11 but rather the sum $F_b - F_{def\_assim} + F_{def\_resp}$, which is not a very useful quantity in global carbon cycle studies. Therefore, Townsend *et al.* (2002) have made implicitly the approximation $F_{def\_assim} \approx F_{def\_resp}$, and therefore:

$$D_{def}(t) = \int_{u=t-\tau}^{u=t} F_{def\_resp}(\delta_{def\_resp} - \delta_{def\_assim})\,du \tag{14.17}$$

It is also possible without that simplification to rewrite Eq. 14.16 as

$$D_{def} = F_{def\_resp}(t) \cdot (\delta^*_{def\_resp} - \delta^*_{def\_assim}) \tag{14.18}$$

Where:

$$\delta^*_{def\_resp} = \frac{1}{F_{def\_resp}(t)} \int_{t-\tau}^{t} F_{def\_resp}(t') \cdot \delta_{def\_resp}(t') \cdot dt' \tag{14.19}$$

$$\delta^*_{def\_assim} = \frac{1}{F_{def\_resp}(t)} \int_{t-\tau}^{t} F_{def\_assim}(t') \cdot \delta_{def\_assim}(t') \cdot dt' \tag{14.20}$$

with those quantities being flux-weighted by the spatial distribution of F_{def_assim}, F_{def_resp} in the case where a spatially explicit biosphere model is used. The value of D_{def} (Townsend *et al.*, 2002) is -15 GtC ‰ yr^{-1}, that is about one-third of the soil-respired disequilibrium, but of opposite sign. With the land use bookkeeping model of Gitz and Ciais (2003), we performed an independent calculation of D_{def} and obtained -18.9 GtC ‰ yr^{-1}. Both calculations made the same assumption that 80% of deforested areas in the Tropics are replaced by C_4 grasses (50% in Asia because of rice cultivation). Land use changes, yielding to the substitution of forests by C_4 grasslands, mostly occur in the tropics, so adding D_{def} in double deconvolutions increases the tropical sink by roughly 1 GtC yr^{-1} (Townsend *et al.*, 2002).

In addition to tropical land use changes, the establishment of C_4 croplands (maize) at mid-northern latitudes during the twentieth century in North America and Europe has had an impact on the atmospheric $\delta^{13}C$ signal (60 Mha were cultivated for corn in 1980–2000 compared to 2–5 Mha in the early twentieth century). This adds a disequilibrium not accounted for by Townsend *et al.* (2002) that we estimated at 0.5 GtC ‰ yr^{-1} using the simplified land use model (forest–croplands) of Gitz and Ciais (2003). Accounting for additional plowing of grasslands into C_4 croplands in North America would increase that estimate up to 2 GtC ‰ yr^{-1} (M. Scholze, LPJ results, unpublished).

Rock Weathering ^{13}C Isotope Effects

Carbonate rock weathering results in small 'background' natural fluxes in the carbon cycle, acting over land as a sink, $-F_{carb\_w}$, of soil CO_2 reacting with $CaCO_3$ capping the Earth's crust to yield dissolved bicarbonates ions:

$$CO_{2(soil)} + CaCO_3 \rightarrow 2HCO_3^- \tag{14.21}$$

The HCO_3^- ions are transported into freshwater systems, where a small fraction may re-precipitate as carbonates, whereas the rest get transported to the coastal seas by rivers, and a sub-fraction of it to the deep ocean.

In the sea, the inverse of reaction 14.21 precipitates $CaCO_3$ in marine sediments, causing a CO_2 source, F_{carb_sw}, to become available to the atmosphere. Regarding the $\delta^{13}C$ transfers in the weathering cycle, the initial sink has a signature, $\delta_{sw\_uptake} = \delta_b$. As soil CO_2 is enriched by 4.4‰ with respect to δ_b, and reaction 14.21 consumes one mole of soil CO_2 for one mole of soil carbonate (at +1‰), the two HCO_3^- ions in reaction 14.21 take an intermediate $\delta^{13}C$ approximately equal to $(\delta_b + 4.4 + 1)/2 \approx -11‰$, a value effectively observed in freshwaters carbonate systems. Once transferred by rivers to the sea, the dissolved HCO_3^- get isotopically diluted with the huge marine bicarbonate reservoir and when CO_2 returns to the atmosphere, fractionation occurs to reconstitute the isotopic balance. Yet overall, carbonate rock weathering results in the lateral displacement of isofluxes, with an iso-uptake over land of:

$$-F_{carb\_sw} \cdot \Delta_b^{13} \tag{14.22}$$

compensated by an equivalent iso-release over the oceans.

Parallel to the weathering of carbonates, the weathering of silicate rocks proceeds by the reaction:

$$3H_2O + 2CO_2 + MSiO_3 \rightarrow M^{2+} + 2HCO_3^- + H_4SiO_4 \tag{14.23}$$

Once delivered to the ocean via rivers, the two bicarbonates produced by reaction 14.23 contribute to the formation of marine carbonates:

$$2HCO_3^- \rightarrow CaCO_3 + CO_2 \tag{14.24}$$

Unlike for carbonate weathering where the land sink balances an ocean source, for silicate weathering, two moles of atmospheric CO_2 are consumed on land for only one being released over the ocean. The carbon cycle gets balanced over geologic timescales (>1 Myr) since carbonates deposited at the bottom of the sea get subducted in the hot mantle, yielding carbon outgassing by volcanoes. The overall isoflux due to silicate rock weathering can be expressed as:

$$D_{silicate\_weath} = F_{silicate\_weath}(\delta_{sw\_release} - 2 \cdot \delta_{sw\_uptake}) + F_{volcanoes}\delta_{mantle} \tag{14.25}$$

With $F_{silicate\_weath} = 0.2\,\mathrm{GtC\,yr^{-1}}$, $F_{volcanoes} = 0.02\,\mathrm{GtC\,yr^{-1}}$, $\delta_{mantle} = +6‰$, this yields $D_{silicate\_weath} = 3.6\,\mathrm{GtC\,‰\,yr^{-1}}$, equivalent to the aliasing effect of a sink of $0.2\,\mathrm{GtC\,yr^{-1}}$ by land ecosystems. Uncertainties are large on this term and there could also be isotopic equilibrium on long timescales. Overall, both carbonate and silicate rock cause an isoflux of $\approx 4\,\mathrm{GtC\,‰\,yr^{-1}}$, mostly a disequilibrium. This would diminish the mean value of the terrestrial sink currently inferred in double deconvolutions by roughly $0.4\,\mathrm{GtC\,yr^{-1}}$. Since 'background' fluxes only evolve on geologic

timescales, they cause a systematic offset to the mean fluxes, but do not affect the interannual variability and secular changes inferred in double deconvolutions.

Isotope Effects from the Oxidation of Reactive Carbon Gases in the Atmosphere

Carbon compounds are released from plants to the atmosphere as non-CO_2 gases (isoprene, terpenes, CH_4, CO, acetone, methanol, ...). Non-CO_2 gases react with OH and O_3 to be oxidized into CO and eventually into CO_2 (a small direct oxidation channel by R-O_2 radicals into CO_2 also exists). Atmospheric CO has a lifetime of a few months and it is, on average, depleted in ^{13}C compared to atmospheric CO_2 (average δ^{13}C-CO $\approx -27‰$ with a range of -20 to $-40‰$, after Bergamaschi *et al.* [2000b]). Using the oxidation reaction $CO + OH \rightarrow CO_2$ in respect of the kinetic isotope effect (fractionation) determined by Röckmann *et al.* (1998) we estimated that CO_2 produced from CO should be enriched by 3‰ globally with regard to the CO atmospheric reservoir: δ^{13}C-CO_2 from CO oxidation, $\delta_{CO\_oxidation} = -27 + 3 = -24‰$. With a total source of carbon produced by CO oxidation of 0.92 GtC yr^{-1} in the atmosphere (Novelli *et al.*, 1995), this yields a net isoflux (not a disequilibrium) of -25.6 GtC ‰. This isoflux is almost entirely compensated for by the fact that part of the *NPP* is not returned to the atmosphere as CO_2, but via emissions of non-CO_2 gases. Globally, the annual growth rates of CO_2 and δ^{13}C-CO_2 in Eqs 14.10 and 14.11 thus already implicitly include the oxidation of non-CO_2 gases ($F_{CO\_oxidation}$). It should, however, be remarked that atmospheric transport models based on space and time gradients in $\delta^{13}C$ and CO_2 to infer regional fluxes may be biased regionally when not accounting for the emission of non-CO_2 carbon gases and the oxidation of CO into CO_2 within the atmosphere.

Atmosphere–Land Fractionation Factor or Discrimination (Δ_b^{13})

Δ_b^{13} is controlled by the photosynthetic pathway (C_3/C_4) and by the ratio of the chloroplast to canopy CO_2 concentration (C_c/C_a). C_3 and C_4 photosynthetic fractionation differences are associated with the biochemical fixation of CO_2; the C_c/C_a ratio depends on the opening of the leaf stomata and therefore is a function of the plant water stress, and of the mesophyll resistance (Lloyd and Farquhar, 1994). The large-scale spatial distribution of Δ_b^{13} reflects mostly the extent of C_4 photosynthesis relative to C_3 (Fig. 14.1) and partly the water limitations for C_3 plants. Figure 14.1 shows two annual maps of Δ_b^{13} as calculated by Scholze *et al.* (2003) using the LPJ terrestrial biosphere model and by Cuntz *et al.* (2003a,b) using the MECBETH photosynthesis–respiration model. Other modelers have produced similar maps of Δ_b^{13} and sometimes calculated the associated

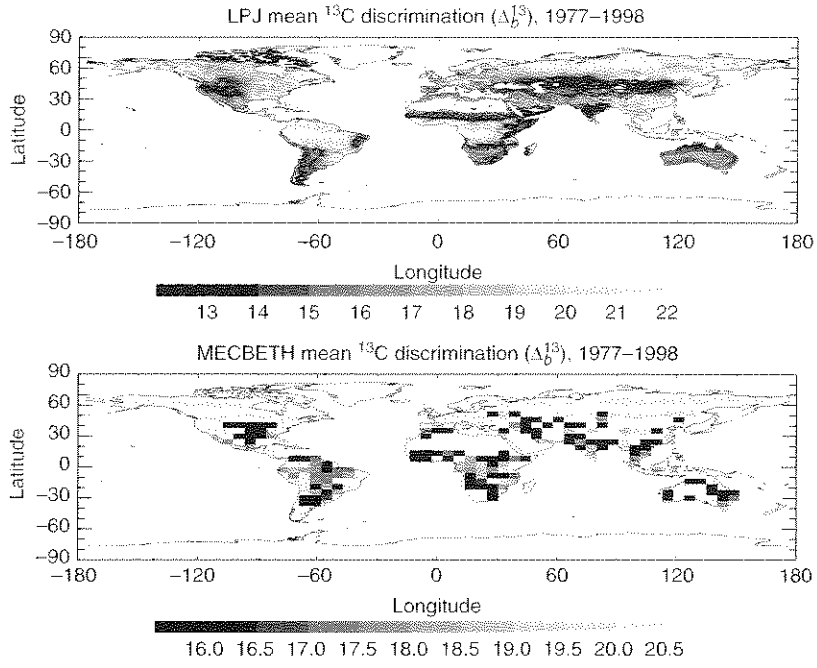

Figure 14.1 Global distribution of photosynthetic discrimination as simulated by two different models: (top) LPJ biogeochemical model at 0.5° spatial resolution forced by climate input data in Scholze *et al.* (2003); (bottom) MECBETH photosynthesis–respiration model coupled to an atmospheric general circulation model at 5° resolution in Cuntz *et al.* (2003a).

$\delta^{13}C$-CO_2 atmospheric distribution using an atmospheric transport model (Fung *et al.*, 1997; Kaplan *et al.*, 2002). Lloyd and Farquhar (1994) mapped Δ_b^{13} by extrapolation of observed physiological relationships. In all these studies, Δ_b^{13} was modeled to vary with latitude across the range from 7 to 10‰ for changes from C_4 to C_3 plants (subtropical to tropical and temperate regions) and from 2 to 4‰ for C_3 plants only (temperate and high latitude regions) reflecting the stomatal response to water stress caused by arid conditions.

It is difficult to validate such Δ_b^{13} maps against observations. Local canopy data are rather scarce and difficult to upscale, although the situation is quickly improving as part of the BASIN and SIBAE isotope networks (see http://basin isotopes.org/ and http://www.esf.org/sibae and references therein). An alternative is to use regional Δ_b^{13} deduced from the relationships between CO_2 and $\delta^{13}C$-CO_2 atmospheric measurements, as did Bakwin *et al.* (1998) and Randerson *et al.* (2002b), but atmospheric measurements are also scarce and difficult to downscale. In Fig. 14.2, we provide such a plot showing different zonally averaged modeled Δ_b^{13} values against atmospheric

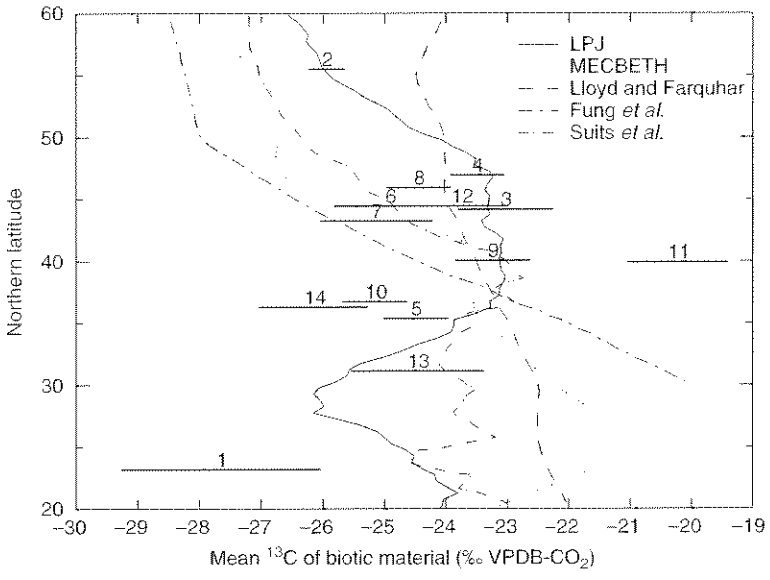

Figure 14.2 Comparison between modeled zonally averaged discrimination north of 20° N (references in the text) and the discriminations inferred from the relationship between CO_2 and $\delta^{13}C$ at atmospheric stations.

station inferred ones. Comparing models with each other yields little information on processes causing differences among them, since the modeled value of Δ_b^{13} is very sensitive to the assumed fractionation parameters (a and b values) as well as to the modeled drop in CO_2 partial pressures between chloroplast (C_c) and leaf stomatal cavity (C_i) corresponding to mesophyll resistance effects.

Temporal variations in Δ_b^{13} relevant to double deconvolution studies occur mainly on an interannual timescale. Year-to-year changes in Δ_b^{13} (as driven for instance by El Niño occurrences) may also possibly covary with photosynthesis to amplify changes in $\delta^{13}C$-CO_2 in Eq. 14.11 both directly through the product $F_b\Delta_b^{13}$ (Randerson *et al.*, 2002a) and indirectly through the disequilibria D_b and D_{bur}. Randerson *et al.* (submitted) calculated that C_4 grasses contribute 31% of global fire emissions, but only 6% of the interannual emission anomalies. Randerson *et al.* (2002b) modeled the interannual changes in the isotopic discrimination of C_3 plants covarying with GPP. Seasonal variations in Δ_b^{13} with an amplitude of 1.8 to 15‰ exist but accompany variations in gross photosynthesis and are not likely to affect inferences from inverse studies (Fung *et al.*, 1997).

There are indications of a long-term trend in the global mean fractionation factor, i.e., a decrease of 0.4‰ during the twentieth century (Scholze *et al.*, 2003); however on the time-span covered by data for atmospheric

inversions (~20 years) such a trend is hardly visible. Two modeling studies found similar amplitudes in the interannual variability of the fractionation factor: less than 1.0‰ (Ito and Oikawa, 2002) and less than 0.3‰ (Scholze *et al.*, 2003). This variability is mainly caused by climate anomalies such as ENSO generally leading to higher plant water stress conditions over tropical forest ecosystems. Although the influence on the partitioning of carbon fluxes is minor compared to the disequilibria term it can lead to biases of 10% in those fluxes.

Understanding $\delta^{18}O$ in Atmospheric CO_2

Carbon dioxide in contact with water can exchange its ^{18}O isotopic signature. If this reaction occurs in nature, in most cases there are several orders of magnitude more water associated than CO_2. That means that the isotopic signature of CO_2 is fully determined by the isotopic signature of the equilibrating water, which is barely changing itself. Due to evaporation, the water in leaves which equilibrates with CO_2 is highly enriched in ^{18}O compared to soil water, which in turn equilibrates with CO_2 leaving the soil from respiration processes. The relevant biosphere CO_2 fluxes are thus the gross fluxes, assimilation and respiration, which determine the $\delta^{18}O$ in atmospheric CO_2. These two gross fluxes are about two orders of magnitude greater than the biospheric net flux. Other CO_2 exchange processes, such as ocean exchange, contribute a small fraction to the total $\delta^{18}O$-CO_2 isoflux. The temporal evolution of $\delta^{18}O$-CO_2 in the atmosphere is therefore mainly the sum of two distinct, opposing isofluxes, from assimilation and respiration respectively. Using this feature, a double deconvolution of $\delta^{18}O$-CO_2 and CO_2 allows determination of the two biospheric CO_2 gross fluxes, provided that the other components can be reasonably estimated. This feature was used locally to determine the gross fluxes over a crop field (Yakir and Wang, 1996) and in a spruce forest (Langendörfer *et al.*, 2002), and to determine the biosphere CO_2 gross fluxes globally (Peylin, 1999). But all these studies pointed out that the estimated gross fluxes are still uncertain and strongly rely on *a priori* information about key parameters that control the computation of the isotopic discriminations. Recent global model studies of $\delta^{18}O$ in atmospheric CO_2 showed that we are not yet able to satisfactorily reproduce the atmospheric $\delta^{18}O$-CO_2 signal with our current knowledge of the $\delta^{18}O$-CO_2 cycle (Peylin, 1999; Cuntz *et al.*, 2003a,b).

For the mass balance of CO_2 (Eq. 14.9), the CO_2 net fluxes of ocean and biosphere can be split into gross fluxes:

$$\frac{dC_a}{dt} = F_o + F_b + F_f = F_{oa} - F_{ao} + F_R - F_A - F_f - F_{bur} \qquad (14.26)$$

where F_{oa} is the flux from the ocean to the atmosphere, F_{ao} the flux from the atmosphere to the ocean, F_R the total respiration flux, and F_A the assimilation flux (all four terms defined as positive values). Biomass burning is thereby not included in the respiration term because, unlike for ^{13}C, it has an isotopic signature significantly different from that for ^{18}O respiration. The global $\delta^{18}O$-CO_2 budget is then (Francey and Tans, 1987; Farquhar *et al.*, 1993; Ciais *et al.*, 1997a,b; Peylin *et al.*, 1997; Tans, 1998):

$$\frac{d\delta_a}{dt} = F_{oa}\Delta_{oa} + F_{ao}\Delta_{ao} + F_R\Delta_R + F_A\Delta_A + (F_f + F_{bur})\Delta_{f,bur} + F_{inv}\Delta_{inv} + F_{strat}\Delta_{strat} \tag{14.27}$$

with

$$\Delta_{oa} = \delta_o + \varepsilon_o - \delta_a \tag{14.28}$$

$$\Delta_{ao} = -\varepsilon_o \tag{14.29}$$

$$\Delta_R = \delta_s + \varepsilon_s - \delta_a \tag{14.30}$$

$$\Delta_A = -\varepsilon_l \frac{C_a}{C_a - C_{cs}} + (\delta_l + \varepsilon_l - \delta_a)\frac{C_{cs}}{C_a - C_{cs}} = -\varepsilon_l + \frac{C_{cs}}{C_a - C_{cs}}(\delta_l - \delta_a) \tag{14.31}$$

$$\Delta_{f,bur} = \delta^{18}_{O_2} - \delta_a \tag{14.32}$$

$$\Delta_{inv} = \delta_s - \delta_a \tag{14.33}$$

$$\Delta_{strat} = \delta_{strat} - \delta_a \tag{14.34}$$

The last two terms in Eq. 14.27 are the isotope effects due to 'invasion' of CO_2 into the soil and to the stratosphere–troposphere gross exchange of CO_2. They can be called 'isotopic disequilibria', as for ^{13}C, because they have no CO_2 counterpart. We will discuss in the following each term of Eq. 14.27 in order to determine its importance for the global budget of $\delta^{18}O$-CO_2, or even regional budget to a lesser extent, and describe how well they are currently known.

As mentioned before, CO_2 equilibrating with water is almost always fully determined by the isotopic composition of the water. This equilibration process is temperature dependent and the fractionation between water and CO_2 equilibrated with water follows the relationship (Brenninkmeier *et al.*, 1983):

$$\varepsilon_{eq}(T) = \left(\frac{17604}{T} - 17.93\right) \Big/ 1000 \tag{14.35}$$

such that CO_2 equilibrated with water has the isotopic composition of:

$$\delta_{CO_2} = \delta_{H_2O} + \varepsilon_{eq} \tag{14.36}$$

The ε's in Eqs 14.28–14.34 are kinetic fractionations and will be dealt with in the following sections.

Air–Sea Isoflux of δ^{18}O-CO_2

The first two terms of Eq. 14.27 can be rewritten in order to separate the effect of the net air–sea flux and that of the ocean-to-atmosphere gross flux:

$$F_{oa}\Delta_{oa} + F_{ao}\Delta_{ao} = F_o\varepsilon_o + F_{oa}(\delta_o - \delta_a) \tag{14.37}$$

The net contribution, usually referred as the equilibrium term, is proportional to the net air–sea exchange, which is of the order of $-2\,GtC\,yr^{-1}$. Given the small kinetic fractionation from diffusion of CO_2 at the air–sea interface, $\varepsilon_o = 0.8‰$ (Vogel *et al.*, 1970), the isoflux is only of the order of $-1.6\,GtC\,‰\,yr^{-1}$ and thus negligible. The second term, usually referred to as the ocean isotopic disequilibrium, tends to adjust the atmospheric δ^{18}O-CO_2 signal towards the δ^{18}O of CO_2 dissolved in ocean surface water, δ_o. This latter is dictated by the isotopic composition of ocean surface water δ_o^w and by the surface temperature through Eqs 14.35 and 14.36. Based on ocean measurement campaigns, Craig and Gordon (1965) proposed an empirical regression that relates the δ^{18}O of H_2O to surface salinity, a relation that has been used by most global studies (Francey and Tans, 1987; Farquhar *et al.*, 1993; Ciais *et al.*, 1997a,b; Peylin *et al.*, 1997; Cuntz *et al.*, 2003a,b): $\delta_o^w = 0.5 \cdot \text{salinity} - 16.75$, with the salinity expressed in ‰ and δ_o^w in ‰ VSMOW. The resulting δ_o^w field decreases towards high latitudes where salinity is lower. Note however that in some particular areas with very low salinity, such as the Baltic Sea, this relation produces too-low values and should thus be corrected (Förstel *et al.*, 1975). The temperature dependence of the fractionation factor ε_{eq} (Eq. 14.37) counterbalances this latitudinal effect and the resulting δ_o field increases from low latitudes toward high latitudes with values around 0 and 6‰ VPDB-CO_2, respectively (Peylin, 1999). Given tropospheric values of δ_a (between -2 and $+2‰$) the overall effect of the air–sea exchange is to enrich the atmosphere in ^{18}O. The amplitude of this effect is directly proportional to the gross sea-to-air flux $F_{oa} = K_{ex}p_o$. Like the case with ^{13}C, the estimation of this isotopic disequilibrium requires the knowledge of the CO_2 partial pressure in surface waters (p_o) and of the air–sea gas exchange transfer coefficient K_{ex}. As mentioned above, F_{oa} increases with time (with an increase of roughly 30% since preindustrial times) and today's average value is of the order of $85 \pm 17\,GtC\,yr^{-1}$ (Heimann and Maier-Reimer, 1996). Weighted according to F_{oa}, the global value of $(\delta_a - \delta_a)$ is around $+0.7$ to $+1.6‰$ (Farquhar *et al.*, 1993; Ciais *et al.*, 1997a,b;

Peylin, 1999; Cuntz *et al.*, 2003a), which in turn would increase δ_a by $\sim 140\,GtC\,‰\,yr^{-1}$. Such a contribution should be accounted for properly in a double deconvolution of $\delta^{18}O$-CO_2 and CO_2 as it corresponds to around $20\,GtC\,yr^{-1}$ of terrestrial respiration. This air–sea isoflux bears also a large uncertainty given the uncertainty of F_{oa} (at least 30% from K_{ex}).

$\delta^{18}O$-CO_2 Isoflux of the Terrestrial Respiration

Carbon dioxide in soil equilibrates isotopically with soil water. But the isotopic composition of soil changes with depth. Ciais *et al.* (1997a) estimated that, on average, a CO_2 molecule can travel about 12 cm in soil before it takes the isotopic signature of water (value adjusted for the correct reaction rate). Miller *et al.* (1999) developed from their measurements the rule of thumb that the relevant water isotopic composition is the one at a depth of 15 cm. Riley *et al.* (2002) compared this with their numerical solution of the diffusion equation of CO_2 in soil and found a good agreement with the 15 cm rule of thumb in most cases. So it is common sense to take the water isotopic composition at 15 cm soil depth for CO_2 equilibration. But Riley *et al.* (2002) recognized in addition strong deviations from the 15 cm rule, for example in semi-arid regions, where high soil evaporation leads to steep water isotope profiles. In regions with high water pressure deficits, the water content near the surface can diminish sharply, coupled with very high $\delta^{18}O$-H_2O values (Mathieu and Bariac, 1996a,b; Melayah *et al.*, 1996). There is then the competition of CO_2 fractionation due to diffusion and CO_2 equilibration with soil water to take into account. Respiration isofluxes, for example in savannas, are therefore most probably erroneously calculated using the simple approach of Eq. 14.30. When CO_2 diffuses out of the soil, it becomes fractionated with a maximum fractionation of $-8.8‰$. In the atmosphere, it will then be transported without fractionation. But CO_2 has to pass an intermediate, laminar air layer just at the ground level where the fractionation is only $-5.9‰$ (Merlivat and Jouzel, 1979). The effective fractionation will be something in between and the most recent estimate of the global mean is $\varepsilon_s = -7.2‰$ (Miller *et al.*, 1999).

The concentration of CO_2 in soil can rise to very high levels in deep soil (Hesterberg and Siegenthaler, 1991). Therefore, the CO_2 flux coming from soil was determined to be a one-way diffusive flux and the flux from the air into the soil was neglected. Tans (1998) showed that the back-diffusion flux should be considered for $\delta^{18}O$-CO_2. He divided the 'net' flux on the ground into the 'normal' CO_2 respiration flux just leaving the soil and a CO_2 flux which enters the soil from the air (with the isotopic signature of atmospheric CO_2), equilibrates with soil water, and leaves the soil again (with the soil water isotopic signature). This effect is called 'invasion' and the flux from air to soil and back to air is called 'invasion flux' (Tans, 1998) or 'abiotic

flux' (Stern *et al.*, 2001). Tans (1998) estimated a global CO_2 invasion flux of roughly $30\,GtC\,yr^{-1}$ from a back-of-the-envelope calculation and Cuntz *et al.* (2003) calculated a global CO_2 invasion flux of $18.6\,GtC\,yr^{-1}$ with a global 3-D model of $\delta^{18}O\text{-}CO_2$.

Soil water integrates precipitation inputs, and likewise the isotopic signature of soil water integrates incoming meteoric water isotopic composition. Annual mean meteoric water over land is around $-7‰$ vs VSMOW (Farquhar *et al.*, 1993; Gat, 2000). The soil seems to damp down, almost completely, incoming meteoric inputs (Yurtsever and Gat, 1981; Hesterberg and Siegenthaler, 1991) but measurements of the isotopic composition of nighttime CO_2 fluxes indicate that soil isotopes could change seasonally by about $10‰$ (Cuntz *et al.*, 2003b). These observations support a mean respiration weighted value of $\delta_s = -6 \pm 2‰$.

$\delta^{18}O\text{-}CO_2$ Isoflux of the Terrestrial Assimilation

To close the $\delta^{18}O\text{-}CO_2$ budget, Francey and Tans (1987) speculated that plants had to assimilate about $200\,GtC\,yr^{-1}$, which seemed unreasonable. But Farquhar *et al.* (1993) showed that the assimilation of CO_2 is a diffusive process and therefore CO_2 enters and leaves the stomata, resulting in a diffusive net CO_2 flux: assimilation, driven by the CO_2 mixing ratio gradient between chloroplasts and canopy air. Plants use the enzyme carbonic anhydrase to accelerate the fixation of CO_2 and therefore Farquhar *et al.* suggested that all CO_2 leaving the stomata by diffusion is isotopically equilibrated with leaf water. The flux from canopy air to the stomata is thus $g_s C_a$ and the flux from the stomata to canopy air $g_s C_{cs}$ (g_s being roughly the stomatal conductance), resulting in assimilation:

$$F_A = g_s(C_a - C_{cs}) = \frac{C_a}{(C_a - C_{cs})} F_A - \frac{C_{cs}}{(C_a - C_{cs})} F_A \qquad (14.38)$$

The value of C_{cs} is about $0.7C_a$, so the first ratio gives about $3F_A$ and the second ratio about $2F_A$. The influx only fractionates kinetically and the outflux is isotopically equilibrated with leaf water, leading to Eq. 14.31. Carbon dioxide from the canopy has to diffuse to the leaf surface, through a laminar boundary layer at the leaf surface (fractionation: $-5.9‰$) and through the stomata (fractionation: $-8.8‰$). Again, the effective fractionation falls somewhere in between. Farquhar *et al.* (1993) estimated a global mean value of $\varepsilon_l = -7.4‰$. But this came from a simple hand calculation and canopy measurements suggest that the effective fractionation could be closer to $-5.9‰$ (Langendörfer *et al.*, 2002).

Carbon dioxide inside the stomata is hydrated very quickly due to the enzyme carbonic anhydrase in the mesophyll cell water. It diffuses next to

the chloroplasts where it enters the Calvin cycle. This is 'driven' by the gradient between the stomata, C_i, and the chloroplasts, C_c. Gillon and Yakir (2000a) claimed that carbonic anhydrase effectively erases the gradient of CO_2 mixing ratios between the stomata and the chloroplasts, leading to a CO_2 mixing ratio which equilibrates with leaf water, C_{cs}, somewhere between C_i and C_c. They suggested that a reasonable assumption would be halfway between the two CO_2 mixing ratios. The average drawdown between C_c and C_i lies between $0.1C_a$ (Lloyd and Farquhar, 1994) and $0.2C_a$ (Yakir and Sternberg, 2000), so Gillon and Yakir (2000a) suggested taking a value of $C_{cs} - C_i = 0.1C_a$. The actual drawdown between stomata and chloroplasts can be calculated if one knows the stomatal and the mesophyll conductances. However, the latter is very hard to measure and hence not very well known (for details see Gillon and Yakir, 2000a).

There is also a difference between leaf water isotopic composition at the surface of the mesophyll cells, δ_l^w, where water is evaporating, and the supplying vein water isotopes, δ_s^w. Craig and Gordon (1965) developed a formulation for the isotopic composition of evaporative water. When the isotopic composition of water vapor flux becomes stationary, it tends towards the isotopic composition of the supplying water δ_s^w (Bariac *et al.*, 1990), which is an approximately root-density weighted mean of soil water (Bariac *et al.*, 1987; Bariac, 1988). This formulation is called the Craig and Gordon equation and in a simplified form is:

$$\delta_{l-CG}^w = \delta_s^w + \varepsilon_l^w - \varepsilon_k^w + h(\delta_s^w + \varepsilon_k^w - \delta_a^w) \tag{14.39}$$

The superscript w denotes thereby that water isotopes are involved. ε_l^w is the equilibrium fractionation between water and water vapor, ε_k^w the kinetic fractionation from the site of evaporation to canopy air, h the relative humidity normalized to leaf temperature, and δ_a^w the isotopic composition of water vapor in the canopy. But this formulation assumes steady state conditions that are probably not achieved in nature very often (Roden and Ehleringer, 1999; Barbour *et al.*, 2000). Modifying the Craig and Gordon formulation to non-steady state conditions leads to transitional models where one has to make certain assumptions. Assuming a well-mixed leaf water pool of composition δ_s^w which is not changing over time, this results in the transitional model of leaf water at the evaporating site (Förstel *et al.*, 1975):

$$\delta_l^w|_t = \delta_l^w|_{t-1} - (\delta_l^w|_{t-1} - \delta_{l-CG}^w|_t)\exp\{-\Delta t/\tau\} \tag{14.40}$$

with $\delta_l^w|_t$ the leaf water isotopic composition at timestep t and that $\delta_l^w|_{t-1}$ that at timestep $t-1$; τ the turnover time of leaf water corrected for isotope fractionation, $\tau = \zeta V_l/E_v$ with $\zeta = (1-h)(\varepsilon_l^w + 1)(\varepsilon_k^w + 1)$; V_l the leaf water volume; and E_v the transpiration rate. So, leaf water tends to the steady state but only reaches it if evaporation is very high. But this formulation neglects

the existence of a gradient in leaf water isotopic composition from incoming source water to the site of evaporation (Péclet effect; Farquhar and Lloyd (1993); and also neglects the fact that the source water can change its isotopic composition during the day. Nevertheless, the transitional model builds a lower limit and the Craig and Gordon model an upper limit for leaf water isotopic composition. Farquhar *et al.* (1993) calculated a global mean Craig and Gordon value of $\delta_l^w = 4.4‰$ (vs VSMOW) and Ciais *et al.* (1997a) a value of around 3‰. Neither used the transitional model but they calculated their estimates on a monthly basis which (almost) averages out the differences between the Craig and Gordon formulation and the transitional model. Cuntz *et al.* (2003b) included a diurnal cycle in the calculation of Craig and Gordon and the transitional model and calculated a difference of 1‰ between the two formulations, as assimilation-weighted values. They estimated a non-assimilation-weighted Craig and Gordon value of 5.6‰, which is already higher than the estimates of Farquhar *et al.* (1993) or Ciais *et al.* (1997a). Using assimilation-weighted values increased the Craig and Gordon result markedly (7.0‰), but the transitional model in contrast diminished the actual δ_l^w to 6.3‰. These estimates seem to be more realistic because they also fit better with estimates of δ_l^w from the global isotope budget of O_2 (Bender *et al.*, 1994).

Recently, it was doubted that CO_2 leaving the stomata by diffusion is always in isotopic equilibrium with leaf water (Gillon and Yakir, 2000b, 2001). This could be due to reduced activity of the enzyme carbonic anhydrase but also due to the diffusive nature inside the stomata. Gillon and Yakir added an extra term to Eq. 14.33, Θ, the fraction of CO_2 molecules which become hydrated in leaf water. This term effectively reduces Δ_A.

$$\Delta_A = -\varepsilon_l + \frac{C_{cs}}{C_a - C_{cs}}(\delta_l - \delta_a) - \frac{C_{cs}}{C_a - C_{cs}}(1 - \Theta)(\delta_l - \delta_a - [1 - C_{cs}/C_a]\varepsilon_l) \tag{14.41}$$

This seems to be mostly important for C_4 plants, C_4 grasses for example having $\Theta = 0.4$, whereas C_3 plants have values of $\Theta = 0.9$ or higher. Gillon and Yakir (2001) estimate a global mean value of 0.78 and Cuntz *et al.* (2003b) estimate 0.8, where differences derive only from the different vegetation distribution used.

δ^{18}O-CO_2 Isoflux of Burning Processes

Burning processes transform carbonaceous material and atmospheric oxygen into CO_2. It is assumed that the newly formed CO_2 bears the isotopic signature of atmospheric oxygen: $\delta_f = -17‰$ (Kroopnick and Craig, 1972). To our knowledge, there are no observations of this value for different

burning processes, and it could potentially be different for specific burning processes. As detailed above for ^{13}C, burning occurs over very different areas of the world but mainly involves tropical forest and savannas with a global total of 2 to 3.4 GtC yr^{-1} (Table 14.1). This source of carbon is partially offset by a carbon sink due to re-growth over burned areas (F_{bur_regrow} term in ^{13}C section). Such an offset concerns essentially tropical savannas with values of the order of 0.36 GtC yr^{-1}, 1.04 GtC yr^{-1}, and 0.1 GtC yr^{-1} for South America, Africa, and South Asia, respectively. These estimates are based on the difference between the burning flux of Hao *et al.* (1990) and the net deforestation flux of Houghton (1999). In Africa, 75% of the CO_2 emitted from biomass burning is reincorporated within the same year by re-growth of savannas while the fractions in South America and South Asia are only 35% and 15%, respectively. For these latter regions, it implies a large loss of carbon. The effect of re-growth should be treated as a $\delta^{18}O\text{-}CO_2$ isoflux of terrestrial assimilation (see above). However, at a global scale the re-growth concerns only a small amount of carbon compared to the gross assimilation flux F_A, so its isoflux will not significantly impact a double deconvolution of $\delta^{18}O\text{-}CO_2$ and CO_2.

Stratosphere to Troposphere $\delta^{18}O\text{-}CO_2$ Isoflux

Carbon dioxide in the stratosphere is enriched by 2–3‰ in ^{18}O compared to the troposphere (Gamo *et al.*, 1989) due to isotopic exchange of CO_2 with mass-independently enriched ozone in the stratosphere (Thiemens, 1999). Carbon dioxide enters the stratosphere mainly in the tropics and this flux is mostly counterbalanced by a CO_2 flux from the stratosphere to the troposphere in the extra-tropics (Zahn *et al.*, 1999, 2000). This leads to a contribution of the stratosphere–troposphere exchange (STE) to the north–south gradient in tropospheric $\delta^{18}O\text{-}CO_2$ (Peylin *et al.*, 1997). STE is assumed to have a gross CO_2 flux of about 200 GtC yr^{-1} (Hesshaimer, 1997), which leads to an isoflux of about 400 GtC ‰ yr^{-1}. Because the STE is strongest in spring in the northern hemisphere, STE could also lead to seasonal variations in the tropospheric $\delta^{18}O\text{-}CO_2$ signal. But until now, this flux has not been estimated reliably and is a major unknown in the global $\delta^{18}O\text{-}CO_2$ cycle.

Concluding Remarks

The apportionment of sources and sinks between ocean and land using $\delta^{13}C$ and CO_2 records in the atmosphere is mainly dependent on isotopic disequilibrium terms, which have an impact on the atmospheric trend as large as the net fluxes themselves. At the global scale, isotopic

Table 14.1 Estimates of Carbon Emissions due to Biomass Burning (TgC yr^{-1}) and their Isotopic $\delta^{13}C$ Signature (‰ PDB) for the Major Ecosystems (TgC = 10^{12}G+C)

	Average carbon emission by fires (TgC yr^{-1})	Average fire return interval (yr)	References	Average $\delta^{13}C$ of burned biomass (‰ PDB)
Tropical forest	600–1000	250 (100–500)	Levin (1994)	
	(200–1200) (Amazonia alone)		Cochrane and Laurence (2002) Potter *et al.* (2001)	
Mixed forest	38 (11–60) USA	100	Leenhouts (1998)	−7.03
	17 (10–49) China	20–120	Wang *et al.* (2001)	−7.03
	8 Europe (mostly Mediterranean)	10–110	Mouillot *et al.* (2002)	−7.17
	22 Australia	30	Trabaud (1994) Gill *et al.* (1997)	−7.57
Boreal forest	40 (10–100) Canada	200	Chen *et al.* (2000)	−6.76
	50 (10–100) Russia	50 (25–100)	Shvidenko and Nilsson (2000) Conard and Ivanova (1997)	−7.32
Grasslands Savanna	1100 (500–1200) Africa	3	Barbosa *et al.* (1999)	−7.91
	82 India	3	Hao and Liu (1994)	−7.91
	550 South America	5	Seiler and Crutzen (1980)	−7.88
	100 (70–150) Australia	4		−7.90
	66 Central Asia	10		−7.83
Agriculture	910	1	Andreae (1991)	−8
Total	(2081–3449)			−7.46

Today's atmosphere is set to −8‰ and ice core data have been used in this calculation. Averages and minimum/maximum values (in brackets when available) are presented.

disequilibria have an uncertainty range of 30% for the air–sea disequilibrium (range 47–60 GtC ‰ yr^{-1}) and 50% for the soil-respired disequilibrium (range 19.8–33.6 GtC ‰ yr^{-1}). Further, we have quantified other important disequilibrium and isofluxes, which are generally ignored in double deconvolutions:

(1) The replacement of C_3 by C_4 vegetation, which amounts to 50–100% of the soil respiration disequilibrium but has an opposite sign (−15 to −22 GtC ‰ yr^{-1}).
(2) The (small) disequilibrium induced by biomass burning processes (1.7 GtC ‰ yr^{-1}).
(3) The disequilibrium of rock weathering processes (10.5 GtC ‰ yr^{-1}).
(4) The correction to soil-respired disequilibrium due to non-CO_2 gas emissions and oxidation within the atmosphere (17 GtC ‰ yr^{-1}).

At the regional level, some isotopic disequilibrium can become proportionally larger than the isoflux of net CO_2 fluxes, especially at high northern latitudes for the aging of soil-respired CO_2, and in the Tropics for the shifts from C_3 to C_4 vegetation. At even smaller scales, the ecosystems are probably never approaching isotopic equilibrium, neither over long timescales because of disturbances (biomass formed never has the same age as soil-respired carbon), nor on very short timescales (the isotopic composition of photosynthates does not equal that of respiration). Over time, interannual climate-induced fluctuations in the biospheric fractionation factor alter the interference of land and ocean sinks anomalies using atmospheric records of $\delta^{13}C$ and CO_2 by less than 0.1 GtC yr^{-1}. On the other hand, the C_3 shift to C_4 land use-induced disequilibrium should not change strongly from one year to the next; neither should the disequilibrium due to rock weathering. The soil-respired and air–sea isotopic disequilibrium should have a rate of interannual variability similar to one of gross fluxes, that is 10–20% globally, according to terrestrial and ocean model calculations. Priorities in future research should be to include all disequilibria in inverse atmospheric transport models to re-analyze regional fluxes. As recently performed for $C^{18}O$ by Cuntz *et al.* (2003a,b), it should also be important to incorporate 'on-line' the discrimination of $^{13}CO_2$ by canopy photosynthesis and its subsequent transport in the atmosphere in coupled land-surface–atmosphere models.

For $\delta^{18}O$-CO_2, the atmospheric transport and the biospheric $\delta^{18}O$-CO_2 isofluxes determine almost completely the atmospheric signal (see Table 14.2). $\delta^{18}O$-CO_2 has therefore a high potential to deduce the CO_2 gross fluxes of the terrestrial biosphere, but the ^{18}O isotopic exchange between water and CO_2 makes the $\delta^{18}O$-CO_2 cycle more complex than the $\delta^{13}C$ cycle. On the other hand, $\delta^{18}O$ in atmospheric CO_2 is determined by the gross fluxes of the carbon cycle compared to $\delta^{13}C$ that is determined

Table 14.2 Global δ^{18}O-CO_2 Isofluxes of Different Processes[a]

Process	Isoflux (GtC ‰ yr^{-1})
Assimilation	600–1850
Respiration	−600– −1450
Ocean net flux	1.5–2
Ocean gross flux	70–160
Fossil fuel	~−100
Biomass burning	~−50
Invasion	~−130
Stratosphere	200–400
Carb. anhydrase	~−300

[a]Estimated from Peylin (1999) and Cuntz *et al.* (2003a,b).

by the net fluxes. Isotopic disequilibria play therefore an important role in the δ^{13}C cycle but are of secondary importance for δ^{18}O-CO_2. The main unknown in the δ^{18}O-CO_2 cycle is leaf discrimination (Δ_A) due to large uncertainties in its determining variables: mainly the relevant CO_2 mixing ratio inside the leaf (C_{is}), the leaf water isotopic composition at the site of evaporation (δ_l^w), and the carbonic anhydrase activity. Global estimates for leaf water isotopic composition range between 3 and 8.8‰ VSMOW (Gillon and Yakir, 2001) and lead to an uncertainty in Δ_A of about 25%. This puts a limit to the accuracy at which the assimilation can currently be retrieved in double ^{18}O deconvolutions. The stratosphere–troposphere exchange is the other important uncertain term in the δ^{18}O-CO_2 cycle. The stratosphere contributes most probably an isoflux of about 400 GtC ‰ yr^{-1} to the troposphere, which is approximately one fourth of the assimilation isoflux. Not taking it into account in double ^{18}O deconvolutions would lead to a similar bias in the derived terrestrial biosphere CO_2 gross fluxes to that caused by the uncertainty in Δ_A. The contribution of the mass-independent enrichment of δ^{18}O-CO_2 in the stratosphere has not yet been incorporated in global models because of the low vertical resolution of the models and it was speculated that this could lead to the observed differences between modeled and measured δ^{18}O-CO_2 at observatories of marine background air (Cuntz *et al.*, 2003b).

Notations

C_a atmospheric CO_2 mixing ratio
C'_a atmospheric $^{13}CO_2$ or $CO^{18}O$ mixing ratio

C_c	CO_2 mixing ratio in chloroplasts
C_{cs}	CO_2 mixing ratio at chloroplast surface
C_i	CO_2 mixing ratio inside stomatal cavity
D	isotopic disequilibria
D_b	soil-respired isotopic disequilibrium
D_{bur}	biomass burning isotopic disequilibrium
$D_{carbonate\_weath}$	carbonate weathering isotopic disequilibrium
D_{def}	land use-induced isotopic disequilibrium
D_o	air–sea isotopic disequilibrium
$D_{silicate\_weath}$	silicate weathering isotopic disequilibrium
E_V	transpiration rate
F	CO_2 flux
F'	$^{13}CO_2$ or $CO^{18}O$ flux
F_A	CO_2 net assimilation
F_{ab}	atmosphere–biosphere CO_2 exchange flux
F_{ao}	atmosphere–ocean CO_2 exchange flux
F_b	biospheric CO_2 net flux
F_{ba}	biosphere–atmosphere CO_2 exchange flux
F_{bur}	biomass burning CO_2 flux
F_{bur_regrow}	CO_2 flux of recovering ecosystem after fire
F_{carb_w}	soil CO_2 uptake with $CaCO_3$
$F_{CO\_oxidation}$	CO_2 produced from CO oxidation
F_{def_assim}	photosynthetic CO_2 uptake of new biomes after deforestation
F_{def_resp}	immediate and delayed CO_2 release from deforestation
F_f	CO_2 release by burning of fossil fuels
F_{HR}	heterotrophic respiration
F_{inv}	invasion or abiotic CO_2 flux
F_o	air–sea CO_2 net flux
F_{oa}	ocean–atmosphere CO_2 exchange flux
F_R	CO_2 net ecosystem respiration
F_{res}	residual terrestrial CO_2 flux, often referred to 'missing sink'
$F_{silicate\_weath}$	CO_2 uptake from silicate rock weathering
F_{strat}	stratosphere–troposphere CO_2 exchange flux
$F_{volcanoes}$	CO_2 outgassed by volcanoes
g_s	stomatal conductance
h	relative humidity
K_{ex}	air–sea gas transfer coefficient
$KIE(\delta^{13}C\text{-}CO)$	kinetic isotope effect (fractionation) of $CO + OH \rightarrow CO_2$

M_a	conversion factor between fluxes in GtC and mixing rations in ppm
NPP	Net Primary Productivity
p	atmospheric pressure
p_a	atmospheric CO_2 partial pressure
p_o	ocean surface CO_2 partial pressure
R	$^{13}C/^{12}C$ or $^{18}O/^{16}O$ isotope ratio
R_a	isotope ratio of atmospheric air
T	absolute temperature
V_l	leaf water volume
δ	relative deviation of isotope ratio from standard material
δ_a	isotopic composition of atmospheric CO_2
δ_a^w	isotopic composition of atmospheric water vapor
δ_b	isotopic composition of soil-respired CO_2 from previously formed biomass
δ_b^r	isotopic composition of soil-respired CO_2 from recently formed biomass
δ_{burn}	isotopic composition of burned material in absence of isotopic fractionation associated with combustion
δ_{burn_regrow}	isotopic composition of recovering ecosystems after fire
$\delta_{CO\_oxidation}$	$\delta^{13}C$-CO_2 from CO oxidation
δ_{def_assim}	isotopic composition of photosynthetic flux of new biomes after deforestation
$\delta^*_{def\_assim}$	apparent isotopic composition of photosynthetic flux of new biomes after deforestation
δ_{def_resp}	isotopic composition of immediate and delayed CO_2 release from deforestation
$\delta^*_{def\_resp}$	apparent isotopic composition of immediate and delayed CO_2 release from deforestation
δ_f	isotopic composition of CO_2 released from burning fossil fuel
δ_{in}	δ-value of flux to the atmosphere
δ_l	isotopic composition of CO_2 equilibrated with leaf water at the evaporation site
δ_l^w	isotopic composition of leaf water at the evaporation site
$\delta_{l\_CG}^w$	steady-state isotopic composition of leaf water at the evaporation site after Craig and Gordon formulation
δ_{mantle}	isotopic composition of CO_2 released from volcanoes

δ_o	isotopic composition of CO_2 equilibrated with ocean surface water
δ_o^e	hypothetical isotopic composition of CO_2 if ocean in isotopic equilibrium with today's atmosphere
δ_o^w	isotopic composition of ocean surface water
δ_{out}	δ-value of flux from the atmosphere
$\delta_{O_2}^{18}$	isotopic composition of atmospheric oxygen
δ_s	isotopic composition of CO_2 equilibrated with soil water
δ_s^w	isotopic composition of soil water
δ_{strat}	isotopic composition of stratospheric CO_2
$\delta_{w\_release}$	isotopic composition of CO_2 released from rock weathering
δ_{w_uptake}	isotopic composition of CO_2 uptake by rock weathering
Δ	discrimination; here difference between flux and atmospheric isotopic composition
Δ_A	^{18}O discrimination of assimilation
Δ_{ao}	^{18}O discrimination of CO_2 entering the ocean from the atmosphere
Δ_b^{13}	^{13}C discrimination of plants
Δ_{b-C_3}	^{13}C discrimination of C_3 plants
Δ_{b-C_4}	^{13}C discrimination of C_4 plants
Δ_{f_bur}	^{18}O discrimination of burning processes
Δ_{inv}	apparent ^{18}O discrimination of invasion (abiotic) CO_2 flux
Δ_{oa}	^{18}O discrimination of CO_2 leaving the ocean to the atmosphere
Δ_R	^{18}O discrimination of respiration
Δ_{strat}	^{18}O discrimination of stratosphere–troposphere exchange
ε	fractionation
ε_{ab}	^{13}C atmosphere–plant equilibrium fractionation
ε_{ao}	^{13}C fractionation of CO_2 entering the ocean
ε_{eq}	^{18}O fractionation effect of CO_2 equilibrating isotopically with water
ε_k^w	kinetic fractionation of water during evaporation
ε_l	^{18}O diffusion fractionation of CO_2 through the stomata
ε_l^w	equilibrium fractionation between water and water vapor
ε_o	^{18}O diffusion fractionation of CO_2 at air–sea interface
ε_{oa}	^{13}C sea-to-air fractionation
ε_s	^{18}O diffusion fractionation of soil respiration
Θ	fraction of CO_2 hydrated in leaf water
τ	turnover time of leaf water corrected for isotope fractionation
ζ	$= (1 - h)(\varepsilon_l^w + 1)(\varepsilon_k^w + 1)$

References

Andreae M. O. (1991) Biomass burning: its history, use, and distribution and its impact on environmental quality and global climate. In *Global Biomass Burning: Atmospheric, Climatic and Biospheric Implications* (J. S. Levine, ed.). MIT Press, Cambridge.

Balesdent J. and Recous S. (1997) Les temps de résidence du carbone et le potentiel de stockage de carbone dans quelques sols cultivés français. *Can J Soil Sci* **77**: 187–193.

Bakwin P., Tans P., White J. W. C. and Andres R. J. (1998) Determination of the isotopic ($^{13}C/^{12}C$) discrimination by terrestrial biology from a global network of observations. *Global Biogeochem Cycles* **13**(3): 555–562.

Barbosa P. M., Stroppiana D. and Gregoire J. M. (1999) An assessment of vegetation fire in Africa (1981–1991): burned areas, burned biomass, and atmospheric emissions. *Global Biogeochem Cycles* **13**: 933–950.

Barbour M. M., Schurr U., Henry B. K., Chin Wong S. and Farquhar G. D. (2000) Variation in the oxygen isotope ratio of phloem sap sucrose from castor Bean. Evidence in support of the Péclet effect. *Plant Physiol* **123**: 671–680.

Bariac T. (1988) Les isotopes stables (^{18}O, ^{2}H) de l'eau dans le continuum sol–plante–atmosphere: Conséquence pour la vapeur d'eau atmosphérique. Doctorate, state thesis (in French), University of Paris, VI.

Bariac T., Klamecki A., Jusserand C. and Letolle R. (1987) Evolution de la composition isotopique de l'eau (^{18}O) dans le continuum sol–plante–atmosphere (exemple d'une parcelle cultivée en blé, Versailles, France, Juin (1984))—Part A. *Catena* 14: 55–72.

Bariac T., Jusserand C. and Mariotti A. (1990) Evolution spatio-temporelle de la composition isotopique de l'eau dans le continuum sol–plante–atmosphère. *Geochim Cosmochim Acta* **54**: 413–424.

Battle M., Bender M. L., Tans P. P., White J. W. C., Ellis J. T., Conway T. and Francey R. J. (2000) Global carbon sinks and their variability inferred from atmospheric O_2 and $\delta^{13}C$. *Science* **287**: 2467–2470.

Bender M., Sowers T. and Labeyrie L. (1994) The Dole effect and its variations during the last 130 000 years as measured in the Vostok ice core. *Global Biogeochem Cycles* **8**(3): 363–376.

Bergamaschi P., Hein R., Brenninkmeijer C. A. M. and Crutzen P. J. (2000b) Inverse modeling of global CO cycle—2, Inversion of $^{13}C/^{12}C$ and $^{18}O/^{16}O$ isotopes ratios. *J Geophysical Res* **105**: 1929–1945.

Bousquet P. (1999a) Inverse modeling of annual atmospheric CO_2 sources and sinks—Part 1: Method and control inversion. *J Geophysical Res* **104**(D121): 26161–26178.

Bousquet P. (1999b) Inverse modeling of annual atmospheric CO_2 sources and sinks—Part 2: Sensitivity study. *J Geophysical Res* **104**(D121): 26179–26193.

Bowling D., Baldocchi D. D. and Monson R. K. (1999) Dynamics of isotopic exchange of carbon dioxide in a Tennessee deciduous forest. *Global Biogeochem Cycles* **13**(4): 903–922.

Bowling D., Tans P. P. and Monson R. K. (2001) Partitioning net ecosystem carbon exchange with isotopic fluxes of CO_2. *Global Change Biol* **7**: 127–145.

Brenninkmeier C. A. M., Kraft P. and Mook W. G. (1983) Oxygen isotope fractionation between CO_2 and H_2O. *Isotope Geosci* **1**: 181–190.

Chen J., Chen W., Liu J. and Cihlar J. (2000) Annual carbon balance of Canada's forests during 1895–1996. *Global Biogeochem Cycles* **14**: 839–849.

Ciais P., Tans P. P., Trolier M., White J. W. C. and Francey R. J. (1995a) A large northern hemisphere terrestrial CO_2 sink indicated by the $^{13}C/^{12}C$ ratio of atmospheric CO_2. *Science* **269**: 1098–1102.

Ciais P., Tans P. P., White J. W. C., Trolier M., Francey R. J., Berry J. A., Randall D. A., Sellers P. J., Collatz J. G. and Schimel D. S. (1995b) Partitioning of ocean and land uptake of CO_2 as inferred by $\delta^{13}C$ measurements from the NOAA Climate Monitoring and Diagnostic Laboratory Global Air Sampling Network [CO_2-$\delta^{13}C$]. *J Geophysical Res* **100**(D3): 5051–5070.

Ciais P., Denning A. S., Tans P. P., Berry J. A., Randall D. A., Collatz J. G., Sellers P. J. *et al.* (1997a) A three dimensional synthesis study of $\delta^{18}O$ in atmospheric CO_2. Part 1. Surface fluxes. *J Geophys Res* **102**(D15): 5857–5871.

Ciais P., Tans P. P., Denning A. S., Francey R. J., Trolier M., Meijer H. J., White J. W. C. *et al.* (1997b) A three dimensional synthesis study of $\delta^{18}O$ in atmospheric CO_2. Part 2. Simulations with the TM2 transport model. *J Geophysical Res* **102**(D5): 5873–5883.

Ciais P., Friedlingstein P., Schimel D. S. and Tans P. P. (1999) A Global calculation of the $\delta^{13}C$ of soil respired carbon: Implications for the biospheric uptake of anthropogenic CO_2. *Global Biogeochem Cycles* **13**(2): 519–530.

Cochrane M. A. and Laurence W. F. (2002) Fire as a large scale edge effect in Amazonian forests. *J Tropical Ecol* **18**: 311–325.

Conard S. G. and Ivanova G. A. (1997) Wildfire in Russian boreal forests—potential impacts of fire regime characteristics on emissions and global carbon balance estimates. *Environ Pollut* **98**: 305–313.

Craig H. and Gordon A. (1965) Deuterium and Oxygen-18 variations in the ocean and the marine atmosphere. In *Stable isotopes in Oceanic Studies and Paleotemperatures* (L.o.g.a.N. Science, ed.) pp. 9–130. Pisa.

Cramer W., Kicklighter D. W., Bondeau A., Moore B., III, Churkina G., Nemry B., Ruimy A. and Schloss A. L. (1999) and the Participants of the potsdam NPP Model Intercomparaison. Comparing global models of terrestrial net primary productivity (NPP): Overview and key results. *Global Change Biol* **5**(S1): 1–15.

Cramer W., Bondeau A., Woodward F. I., Prentice C., Betts R. A., Brovkin V., Cox P. M. *et al.* (2001) Global response of terrestrial ecosytem structure and function to CO_2 and climate change: Results from six dynamic global vegetation models. *Global Change Biol* **7**(4): 357–374.

Cuntz M., Ciais P., Hoffmann G., Allison C. E., Francey R. J., Knorr W., Tans P. P., White J. W. C. and Levin I. (2003a) A comprehensive global 3D model of $\delta^{18}O$ in atmospheric CO_2—Part 2. Mapping the atmospheric signal. *J Geophysical Res* **108** doi: 10.1029/2002 JD003154.

Cuntz M., Ciais P., Hoffmann G. and Knorr W. (2003b) A comprehensive global 3D model of $\delta^{18}O$ in atmospheric CO_2—Part 1. Validation of surface processes. *J Geophysical Res* **108** doi: 10.1029/2002 JD003153.

Ekblad A. and Högberg P. (2001) Natural abundance of ^{13}C in CO_2 respired from forest soils reveals speed of link between tree photosynthesis and root respirations. *Oecologia* **127**: 305–308.

Farquhar G. D. and Lloyd J. (1993) Carbon and oxygen isotope effects in the exchange of carbon dioxide between terrestrial plants and the atmosphere. In *Stables Isotopes and Plant Carbon—Water Relations.* (J. R. Ehleringer, A. E. Hall, and G. D. Farquhar, eds) pp. 47–70. Academic Press, New York.

Farquhar G. D., Lloyd J., Taylor J. A., Flanagan L. B., Syvertsen J. P., Hubick K. T., Wong S. C. and Ehleringer R. (1993) Vegetation effects on the isotope composition of oxygen in atmospheric CO_2. *Nature* **363**: 439–443.

Förstel H., Putral A., Schleser G. and Leith H. (1975) The world pattern of oxygen-18 in rainwater and its importance in understanding the biogeochemical oxygen cycle. In *Isotope Ratios as Pollutant Source and Behavior Indicators* (IAEA, ed.). IAEA, Vienna.

Francey R. J. and Tans P. P. (1987) Latitudinal variation in oxygen-18 of atmospheric CO_2. *Nature* **327**: 495–497.

Francey R. J., Tans P. P., Allison C. E., Enting I. G., White J. W. C. and Trolier M. (1995) Changes in oceanic and carbon uptake since (1982). *Nature* **373**: 326–330.

Fung I. Y., Field C. B., Berry J. A., Thompson M. V., Randerson J. T., Malmström C. M., Vitousek P. M. *et al.* (1997) Carbon-13 exchanges between the atmosphere and biosphere. *Global Biogeochem Cycles* **11**(4): 507–533.

Gamo T., Susumi M., Sakai H., Nakazawa T., Tanaka M., Honda H., Kubo H. and Itoh T. (1989) Carbon and oxygen isotopic ratios of carbon dioxide of a stratospheric profile over Japan. *Tellus* **41B**: 127–133.

Gat J. R. (2000) Atmospheric water balance—the isotopic perspective. *Hydrol Proc* **14**: 1357–1369.

Gaudinski J. B., Trumbore S. E., Davidson E. A. and Zheng S. (2000) Soil carbon cycling in a temperate forest: Radiocarbon-based estimates of residence times, sequestration rates and partitioning of fluxes. *Biogeochemistry* **51**: 33–69.

Gill A. M., Moore P. H. R., Mc Carthy M. A. and Lang S. (1997) *Contemporary Fire Regimes in the Forests of Southwestern Australia*. CSIRO, Australia Environment, Canberra.

Gillon J. and Yakir D. (2000a) Internal conductance to CO_2 diffusion and $C^{18}O$ discrimination in C_3 leaves—Part A. *Plant Physiol* **123**: 201–213.

Gillon J. and Yakir D. (2000b) Naturally low carbonic anhydrase activity in C_4 and C_3 plants limits discrimination against $C^{18}OO$ during photosynthesis—Part B. *Plant Cell Environ* **23**: 903–915.

Gillon J. and Yakir D. (2001) Influence of carbonic anhydrase activity in terrestrial vegetation on the ^{18}O content of atmospheric CO_2. *Science* **291**: 2584–2587.

Gitz V. and Ciais P. (2003) Land use amplifying effects on future CO_2 levels. *Global Biogeochem Cycles* **17**(1): 1024.

Gruber N. and Keeling C. D. (2001) An improved estimate of the isotopic air–sea disequilibrium of CO_2: Implications for the oceanic uptake of anthropogenic CO_2. *Geophys Res Lett* **28**(3): 555–558.

Gurney K. R., Law R. M., Denning A. S., Rayner P. J., Baker D., Bousquet P., Bruhwiller L. *et al.* (2002) Towards robust regional estimates of CO_2 sources and sinks using atmospheric transport models. *Nature* **415**: 626–630.

Hao W. M., Liu M. H. and Crutzen P. J. (1990) Estimates of annual and regional release of CO_2 and other trace gases to the atmosphere from fires in the Tropics, based on the FAO statistics for the period 1975–1980. In *Fires in the Tropical Biota: Ecosystem Processes and Global Challenges* (G. J. Goldammer, ed.) pp. 440–462, Springer-Verlag, Berlin.

Hao W. M. and Liu M.-H. (1994) Spatial and temporal distribution of tropical biomass burning. *Global Biogeochem Cycles* **8**: 495–503.

Heimann M. and Keeling C. D. (1989) A three-dimentional model of atmospheric CO_2 transport based on observed winds: 2. Model description and simulated tracer experiments. In *Aspects of Climate Variability in the Pacific and the Western Americas* (D. H. Peterson, ed.) pp. 237–276. AGU, Washington, USA.

Heimann M. and Maier-Reimer E. (1996) On the relations between the oceanic uptake of CO_2 and its carbon isotopes. *Global Biogeochem Cycles* **10**(1): 89–110.

Hesshaimer V. (1997) Tracing the Global Carbon Cycle with Bomb Radiocarbon. PhD Thesis (in German). University of Heidelberg.

Hesterberg R. and Siegenthaler U. (1991) Production and stable isotopic composition of CO_2 in a soil near Bern, Switzerland. *Tellus* **43B**: 197–205.

Houghton R. A. (1999) The annual net flux of carbon to the atmosphere from changes in land use 1850–1990. *Tellus* **51B**: 298–313.

Ito A. and Oikawa T. (2002) A simulation model of the carbon cycle in land ecosystems (Sim-CYCLE): A description based on dry-matter production theory and plot- scale validation. *Ecol Modelling* **151**(2–3): 143–176.

Joos F. and Bruno M. (1998) Long-term variability of the terrestrial and oceanic carbon sinks and the budgets of the carbon isotopes ^{13}C and ^{14}C. *Global Biogeochem Cycles* **12**(2): 277–295.

Joos F., Meyer R., Bruno M. and Leuenberger M. (1999) The variability into the carbon sinks as reconstructed for the last 1000 years. *Geophys Res Lett* **26**: 1437–1441.

Kaplan J. O., Prentice C. and Buchmann N. (2002) The stable isotope composition of the terrestrial biosphere: Modelling at scales from the leaf to the globe. *Global Biogeochem Cycles* **16**(4): 1060–1068.

Keeling C. D. (1995) Interannual extremes in the rate of rise of atmospheric carbon dioxide since 1980. *Nature* **375**: 666–670.

Kroopnick P. and Craig H. (1972) Atmospheric oxygen: Isotopic composition and solubility fractionation. *Science* **175**: 54–55.

Langendörfer U., Cuntz M., Clais P., Peylin P., Bariac T., Milyukova I., Kolle O., Naegler T. and Levin I. (2002) Modelling of biospheric CO_2 gross fluxes via oxygen isotopes in a spruce forest canopy: A ^{222}Rn calibrated box model approach. *Tellus* **54B**: 476–496.

Leenhouts B. (1998) Assessment for biomass burning in the conterminous United States. *Conservation Ecology [online]* **2**(1): 1–25.

Levin I. (1994) *The Recent State of Carbon Cycling Through the Atmosphere*. Springer-Verlag, Heidelberg.

Lloyd J. and Farquhar G. D. (1994) ^{13}C discrimination during CO_2 assimilation by the terrestrial biosphere. *Oecologia* **99**: 201–215.

Mathieu R. and Bariac T. (1996a) An isotopic study of water movements in clayey soils under a semiarid climate. *Water Resources Res* **32**: 779–789.

Mathieu R. and Bariac T. (1996b) A numerical model for the simulation of stable isotope profiles in drying soils. *J Geophys Res* **101**: 12685–12696.

Melayah A., Bruckler L. and Bariac T. (1996) Modeling the transport of water stable isotope in unsaturated soils under natural conditions. 2 Comparison with field experiments. *Water Resources Res* **32**: 2055–2065.

Merlivat L. and Jouzel J. (1979) Global climatic interpretation of the deuterium—oxygen 18 relationship for precipitation. *J Geophys Res* **84**: 5029–5033.

Miller J. B., Yakir D., White J. W. C. and Tans P. P. (1999) Measurement of $^{18}O^{16}O$ in the soil–atmosphere CO_2 flux. *Global Biogeochem Cycles* **13**: 761–774.

Mouillot F., Rambal S. and Joffre R. (2002) Simulating the effects of climate change on fire frequency and the dynamics of a Mediterranean Maquis woodland. *Global Change Biol* **8**: 423–437.

Murnane R. J. and Sarmiento J. L. (2000) Roles of biology and gas exchange in determinig the $\delta^{13}C$ distribution in the ocean and the pre-industrial gradient in atmospheric $\delta^{13}C$. *Global Biogeochem Cycles* **14**: 389–405.

Nemani R. R., Keeling C. D., Hashimoto H., Jolly W. M., Piper S. C., Tucker C. J., Myneni R. B. and Running S. W. (2003) Climate-driven increases in global terrestrial net primary production from 1982 to 1999. *Science* **300**: 1560–1563.

Novelli P. C., Conway T. J., Dlugokencky E. J. and Tans P. P. (1995) Recent changes of carbon dioxide, carbon monoxide, and methane in the troposphere and implications for global climate change. *World Meteorol Bull* **44**: 32–37.

Ogée J., Peylin P., Clais P., Bariac T., Brunet Y., Berbigier P., Roche C., Richard P., Bardoux G. and Bonnefond J.-M. (2003) Partioning net ecosystem carbon exchange into net assimilation and respiration using $^{13}CO_2$ measurements: A cost-effective sampling strategy. *Global Change Biogeochem Cycles* **17**: doi: 10.1029/2002/GB001995.

Peylin P. (1999) The Composition of ^{18}O in Atmospheric CO_2: A New Tracer to Estimate Global Photosynthesis. PhD Thesis (in French), University of Paris, VI.

Peylin P., Clais P., Tans P. P., Six K. D., Berry J. A. and Denning A. S. (1997) ^{18}O in atmospheric CO_2 simulated by a 3-D transport model: Sensitivity study to vegetation and soil fractionation factors. *Phys Chem Earth* **21**: 463–469.

Potter C., Brooks-Genovese V., Klooster S., Bobo M. and Torregrosa A. (2001) Biomass burning losses of carbon estimated from ecosystem modelling and satellite data analysis for the Brazilian Amazon region. *Atmos Environ* **35**: 1773–1781.

Raich J. W. and Potter C. S. (1995) Global patterns of carbon dioxide emissions from soils. *Global Biogeochem Cycles* **9**(1): 23–36.

Randerson J. T., Thompson M. V. and Field C. B. (1998) Linking ^{13}C based estimates of land and ocean sinks with predictions of carbon storage from CO_2 fertilization of plant growth. *Tellus* **51B**: 668–678.

Randerson J. T., Collatz G. J., Fessenden J. E., Munoz A. D., Still C. J., Berry J. A., Fung I. Y., Suits N. and Denning A. S. (2001) A possible global covariance between terrestrial gross primary production and ^{13}C discrimination: Consequences for the atmospheric 13C budget and its response to ENSO. *Global Biogeochem Cycles* **16**(4): doi: 10.1029/2001/GB001845.

Randerson J. T., Still C. J., Ballé J. J., Fung I. Y., Donney S. C., Tans P. P., Conway T. J., White J. W. C., Vaughn B., Suits N. and Denning A. S. (2002b) Carbon isotope discrimination of arctic and boreal biomes inferred from remote atmospheric measurements and a biosphere–atmosphere model. *Global Biogeochem Cycles* **16**(3): doi: 10.1029/2002/GB001435.

Randerson J. T., Van der Werf G. R., Collatz G. J., Giglio L., Still C. J., Kasischke E. S., Kasibhatla P., Defries R. S. and Tucker C. J. (2004) Interannual variability in fire emissions from C3 and C4 ecosystems. *Global Change Biol*—Submitted.

Rayner P. J., Enting I. G., Francey R. J. and Langenfelds R. (1999) Reconstructing the recent carbon cycle form atmospheric CO_2, $\delta^{13}C$ and O_2/N_2 observations. *Tellus* **51B**: 213–232.

Riley W. J., Still C. J., Torn M. S. and Berry J. A. (2002) A mechanistic model of $H_2^{18}O$ and $C^{18}OO$ fluxes between ecosystems ant the atmosphere: Model description and sensitivity analyses. *Global Biogeochem Cycles* **16**: doi: 10.1029/2002/GB001878.

Röckmann T., Brenninkmeijer C. A. M., Saueressig G., Bergamaschi P., Crowley J., Fischer H. and Crutzen P. J. (1998) Mass independent fractionation of oxygen isotopes in atmospheric CO due to the reaction CO + OH. *Science* **281**: 544–546.

Roden J. S. and Ehleringer J. R. (1999) Observations of hydrogen and oxygen isotopes in leaf water confirm the Craig–Gordon model under wide-ranging environmental conditions. *Plant Physiol* **120**: 1165–1173.

Schimel D. S., Braswell B. H., Holland B. A., McKeown R., Ojima D. S., Painter T. H., Parton W. J. and Townsend A. R. (1994) Climatic, edaphic and biotic controls over the storage and turnover of carbon in soils. *Global Biogeochem Cycles* **8**: 279–293.

Scholze M., Kaplan J. O., Knorr W. and Heimann M. (2003) Climate and interannual variability of the atmosphere–biosphere $^{13}CO_2$ flux. *Geophys Res Lett* **30**(2): 1097.

Seiler W. and Crutzen P. J. (1980) Estimates of gross and net fluxes of carbon between the biosphere and the atmosphere from biomass burning. *Climatic Change* **2**: 207–247.

Shvidenko A. and Nilsson S. (2000) Fire and the carbon budget of Russian forests. In *Fire, Climate Change and Carbon Cycling in the Boreal Forest* (E. S. Kasischke and B. J. Stocks, eds) doi: 10.1029/2001/GL013454.

Stern L. A., Amundson R. and Baisden W. T. (2001) Influence of soils on oxygen isotope ratio of atmospheric CO_2. *Global Biogeochem Cycles* **15**(3): 753–760.

Tans P. P. (1998) Oxygen isotopic equilibrium between dioxide and water in soils. *Tellus* **50B**: 163–178; Erratum: *Tellus* **50B**: 400.

Tans P. P., Berry J. A. and Keeling R. (1993) Oceanic ^{13}C data: A new window on CO_2 uptake by the oceans. *Global Biogeochem Cycles* **7**: 353–368.

Thiemens M. H. (1999) Mass-independant isotope effects in planetary atmospheres and the early solar system. *Science* **283**: 341–345.

Thompson M. V., Randerson J. T., Malmström C. M. and Field C. B. (1996) Change in net primary production and heterotrophic respiration : How much is necessary to sustain the terrestrial carbon sink? *Global Biogeochem Cycles* **10**(4): 711–726.